Peer-reviewed version available at *Appl. Sci.* **2020**, *10*, 4055; doi:10.3390/app10124055

Article

Assessment of mechanical properties of corroded prestressing strands

Chi-Ho Jeon [1], Cuong Duy Nguyen [1] and Chang-Su Shim [1,*]

[1] A Dept of Civil and Environmental Engineering, Chung-Ang University, Seoul, Korea; chihobeer@cau.ac.kr (C.-H.J.); nguyencuong2892@cau.ac.kr (C.D.N.)

* Correspondence: csshim@cau.ac.kr; Tel.: +82-2-820-5895

Abstract: The corrosion of prestressing steel in prestressed concrete bridges is a critical issue for bridge maintenance. To assess structures with corroded strands, it is necessary to define the mechanical properties of the strands and their influence on the structural behavior. In this study, corroded strands are taken from external tendons in existing bridges and tested to define the effects of corrosion on the tensile properties of the strand. Empirical equations for the tensile strength and ductility of the corroded strand are proposed using test results. The most corroded wire governs the mechanical properties of the strand. Experiments on prestressed concrete beams with a single corroded strand are conducted to investigate the structural behavior. A reduction in the flexural strength and maximum deformation is observed from the experiment. According to the section loss of a wire in a strand and its location in a beam, the flexural capacity can be evaluated using the proposed equation. The reduced ultimate strain of the corroded strand can be the governing factor of the flexural strength.

Keywords: corrosion, prestressed concrete bridge, prestressing steel, section loss, strength, ductility

1. Introduction

The tendon is the most important structural element in prestressed concrete (PSC) girders, and its damage can significantly influence the girder's global behavior. The most critical type of damage in tendons is corrosion, which is difficult to detect through inspection. Corrosion-induced failure is not considered in the design of PSC structures and may cause a sudden collapse of a bridge. Once corrosion is found in the tendon, it is a difficult task to quantify the level of corrosion and its location through the entire length of the tendon. Some of the multiple strands in a tendon are invisible and cannot be observed. Therefore, a method to evaluate the level of corrosion as well as the corresponding mechanical properties of the corroded strands is needed.

In the bridges mentioned in a recent American report [1,2] such as the Niles Channel Bridge, Mid-Bay Bridge, Bob Graham Sunshine Skyway Bridge, and Varina-Enon Bridge, external tendon corrosion occurred within the last 20 years of a relatively short service period. Its causes were mainly infiltration of chloride-contaminated water, insufficient grout filling, and uncertain anchorage closure. When these factors occur together, severe corrosion may result. An uncertain anchorage closure could allow the entrance of water, air, and chloride, and an imperfect grout filling may permit the exposure of internal strands to pollutants, causing corrosion as shown in Fig. 1. According to the case study of Carsana et al. [3], a bridge with tendon fractures caused by corrosion had enough grout filling but owing to the segregation of the grout, severe tendon corrosion occurred within 2 years. Chloride was not detected; however, a high sulfate ion content was found on the surface of the grout, and it is assumed to be the cause of the weakening of the grout segregation and strength.

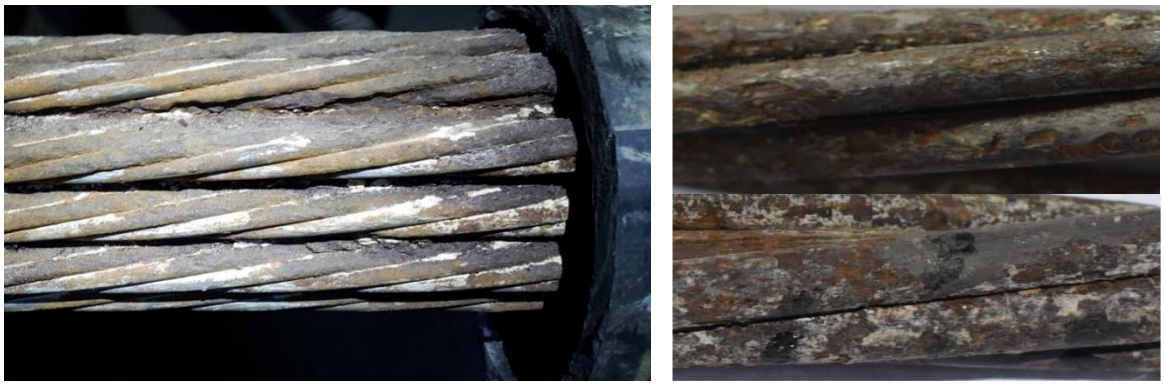

(**a**) (**b**)

Figure 1. Observed corroded strands in existing bridges: (a) Corroded tendon; (b) Corroded strand

Inspections of corroded strands, mostly, have been done for external tendons, because it is easier to observe and replace. Also, it is difficult to repair even if corrosion occurs in inner tendons detected. Therefore, most reports introduced above were focusing on the corrosion of external tendons, and its inspection methods were suggested. Several studies [4-6] have been conducted to evaluate the section loss caused by the corrosion of a strand and the subsequent change in mechanical properties. In all these research studies, the level of corrosion was evaluated using two methods. The first method was to use the loss of mass to evaluate the section loss and apply it to the mechanical property evaluation. This approach used electrochemical methods to induce the corrosion of a strand. The mass loss based on Faraday's law for the evaluation of the chemical reaction of the metal was used as the specimen's damage index in relation to the corrosion. This approach is introduced in ASTM G1-03 [7].

These studies obtained similar results for the decreases in strength and ductility caused by the progression of corrosion. However, there is no viable method to evaluate the corrosion on the strands of an existing PSC bridge. Evaluating the level of corrosion using the mass is not suitable.

The second approach was to use a pit depth gauge to measure the depth of the corrosion pit. The section loss was evaluated using ASTM G49-94 [8] regarding methods to evaluate pitting corrosion. As this approach measures the depth of the corrosion pit, an idealization of the section loss model is needed to quantify the section loss. Many researchers [9~14] suggested section loss models such as the hemispherical and planar pit configurations. Previous research [15] suggested three types of corrosion and their section losses through the observation of corroded strands from PSC bridges. With the help of tests and analyses, the mechanical properties of the corroded strands were determined.

In this study, inspections and tensile experiments were conducted on 100 corroded strand specimens obtained from bridges in service, which were explained in previous studies as well [15, 16]. Based on the experimental results, a reduction in the ultimate strength and fracture strain is suggested in the form of an empirical formula. Flexural tests were also conducted on PSC beams with corroded strands. The behavior of the corroded beams was evaluated, and the suggested equations were verified

2. Investigation of corrosion in external tendons

2.1. Bridge description

Two segmental box girder bridges, located in urban arterial road, that have corrosion in their external strands were examined. Bridge A used 19 seven-wire strands with a nominal diameter of 15.2 mm, while bridge B used 27 seven-wire strands with a nominal diameter of 12.7 mm. A fracture in one external tendon was found 18 years after the bridge construction was completed. The external tendons are covered by a duct filled with grout. To decide on the repair or replacement of the corroded tendons, the ducts were uncovered, and a detailed inspection was conducted. Severe local

section losses were found on the corroded strands. The investigation concluded that the causes were poorly treated air bents and joints in the duct resulting in an infiltration of chloride, presumed to be from de-icing chemicals, and rainwater. In addition, voids not filled by the grout were found inside the duct, and most of the corrosion was located in those sections. In the tendons that were selected for replacement, the corroded strands were cut and moved to a lab to evaluate the corrosion. Tensile tests were conducted on the 100 corroded strands.

2.2. Corrosion inspection

In the corroded strands, owing to corrosion along their length, the pit is very irregular, making it difficult to determine the worst part of the corroded wires by a visual inspection. To quantify the corrosion of the specimen, the ASTM G46-94[8] corrosion measurement method as introduced in a previous study [15] was used. This method uses a pit depth gauge to measure the depth of the pit as shown in Fig. 2; however, this method is unable to evaluate the section loss. Therefore, as in the previous research, a section loss evaluation method using the pit depth was suggested.

Fig. 3 illustrates five cases of corroded strands located near the anchorage and their cut sections. The samples have different levels of corrosion, and the corrosion pits can be easily observed when the corrosion is severe. The five samples were divided into corroded and non-corroded parts. Because a high number of strands exist in a tendon bundle, one portion is exposed to the air, and another portion is in contact with neighboring strands. This results in the corrosion being concentrated on several strands. These samples were not the specimens for the tensile test, because the cut section pictures could not be taken before the tensile test.

Fig. 4 shows an idealized model for the evaluation of each wire's actual section loss pattern and the section loss suggested by previous research. Eqs. (1)–(6) were used for the evaluation of the section loss for each pattern using only the measured pit depth of the corroded strands. This approach does result in errors between the actual and measured corrosion values, but it is the most feasible method for an onsite inspector to evaluate the corrosion, and therefore it is used in this research. The remaining corrosion residue on the extracted specimen was removed by a corrosion removal solution. Then, along the strand's length, the depth of the corrosion was measured every 20 mm using a pit depth gauge as shown in Fig.5. Excluding the core wire, which cannot be evaluated for section loss, the degree of corrosion of each strand was evaluated as the summation of each section loss of the remaining 6 wires as given in Eqs. (1)–(6). The highlighted part in Fig. 5 is the section determined to be the most corroded (the highest section loss) by comparing the summations of the section losses.

Figure 2. Measuring pit depth of corroded wire [15]

Preprints (www.preprints.org) | NOT PEER-REVIEWED | Posted: 20 May 2020 doi:10.20944/preprints202005.0324.v1

Peer-reviewed version available at Appl. Sci. 2020, 10, 4055; doi:10.3390/app10124055

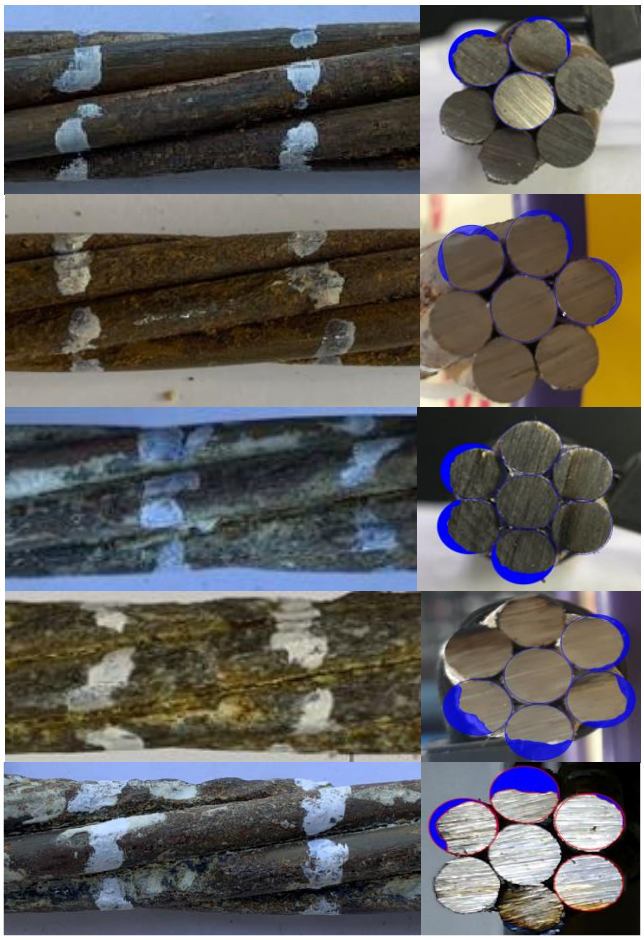

Figure 3. Corrosion of a strand near the anchor in Bridge B

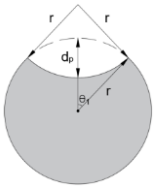

(a) Type 1

$$A_{sl,1} = 2r^2(\theta_1 - sin\theta_1 cos\theta_1) \ for\ 0 \le d_p \le 2r \quad (1)$$

$$\theta_1 = \arccos\left(1 - \frac{d_p}{2r}\right) \quad (2)$$

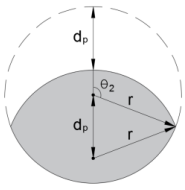

(b) Type 2

$$A_{sl,2} = r^2(2\theta_2 - \pi - 2sin\theta_2 cos\theta_2) \ for\ 0 \le d_p \le 2r \quad (3)$$

$$\theta_2 = \arccos\left(-\frac{d_p}{2r}\right) \quad (4)$$

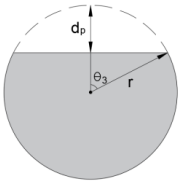

(c) Type 3

$$A_{sl,3} = r^2(\theta_3 - sin\theta_3 cos\theta_3) \ for\ 0 \le d_p \le 2r \quad (5)$$

$$\theta_3 = \arccos\left(1 - \frac{d_p}{r}\right) \quad (6)$$

Figure 4. Pit configurations and equations for section loss calculation [15]

where $A_{sl,1-3}$ are the losses of sectional areas according to the type of pit configuration, r is the radius of the wire, and d_p is the pit depth measured by a depth gauge at the deepest location

Preprints (www.preprints.org) | NOT PEER-REVIEWED | Posted: 20 May 2020 doi:10.20944/preprints202005.0324.v1

Peer-reviewed version available at Appl. Sci. 2020, 10, 4055; doi:10.3390/app10124055

#1		Measured pitting depth (mm)														
Wire \ Distance		20	40	60	80	100	120	140	160	180	200	220	240	260	280	300
1	Pit depth	Invisible core wire														
	Type															
2	Pit depth		0.18				0.60			0.46		0.17	0.35			
	Type		2				3			3		2	2			
3	Pit depth							0.24				0.23		0.35		
	Type							2				2		2		
4	Pit depth			0.12					0.67						0.13	
	Type			2					2						2	
5	Pit depth						0.54					0.56		0.46		
	Type						2					2		2		
6	Pit depth			0.20			0.10		0.15				0.53			
	Type			1			2		2				2			
7	Pit depth				0.23		0.66	0.17	0.25			0.05	0.56			
	Type				2		2	2	2			3	2			

Maximum corroded section

Figure 5. Measured pitting depth of a corroded strand

2.3. Corrosion phenomena in the external tendon

Fig. 6 shows the profile of the voids in the ducts and the number of exposed and corroded strands counted by visual inspection for Bridges A and B. The duct sections not filled by grout were mostly located in upper parts near air bents or anchored at high locations. The void was due to the quality of grout such as bleeding water or from the grout injection process resulting in the strand exposure. Most of the corroded strands were found in a void while strands in the grout in sound condition did not show any corrosion.

Grout samples from the corroded strands in Bridges A and B were analyzed for chemical content (chloride and sulfate), and the section loss due to the corrosion was measured using Eqs. (1)–(6) and Fig. 5. Strands in areas with no grout were not considered. Fig. 7(a) shows the relationship between the section loss and the chloride content percentage with respect to mass of concrete measured by KS F 2713 [17], and Fig. 7(b) shows the relationship between the section loss and the sulfate content measured by KS L 5120 [18]. This demonstrates that the higher the chloride content, the more severe the corrosion, while the sulfate content had a relatively smaller effect on these bridges.

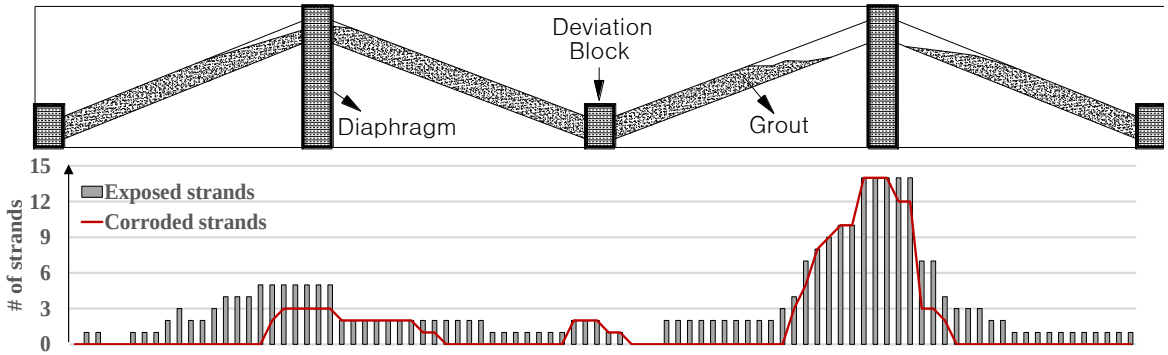

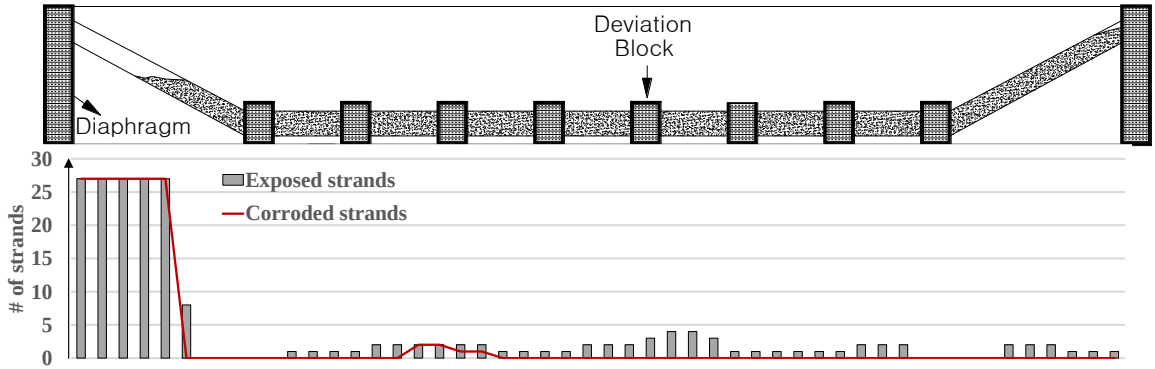

Figure 6. State of grout and corrosion of Bridges A and B

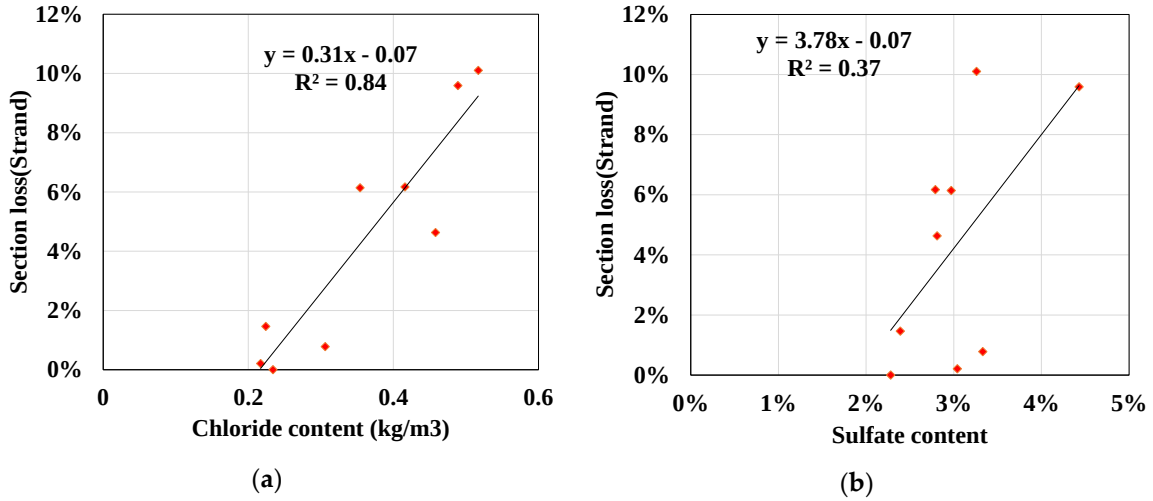

Figure 7. Relationship between chemical state of grout and section loss of strands due to corrosion

3. Tensile test of corroded strand

3.1. Test Specimens

This study complements the previous research [15], and a total of 100 corroded strands were investigated for corrosion. Among the specimens, a total of 86 seven-wire strands (47 strands from Bridge A and 39 strands from Bridge B) were selected for this study excluding specimens that were too corroded to be used in the tensile test. The strands from Bridge A had a nominal diameter of 15.2 mm and a sectional area of 138.7 mm. The radius of the core wire was 2.6 mm, and the radius of the outer wires was 2.5 mm. The strands from Bridge B had a nominal diameter of 12.7 mm and a sectional area of 98.7 mm. The radius of the core wire was 2.2 mm, and the radius of the outer wires was 2.1 mm. In this study, these two strands will be referred to as the 15.2 type and 12.7 type.

Before tests were conducted, the strands were cleaned with a steel brush and rust remover. An inspection to evaluate the section loss was also conducted along the length of the specimen with a pit depth gauge to determine the location of the most corroded section. For the quantitative corrosion comparison, the extent of section loss, denoted as η, is expressed as follows:

$$\eta = \frac{A_{sl}}{A_0}, \tag{7}$$

where A_0 is the sectional area of the wire, and A_{sl} is the loss of the sectional area from Eqs. (1)–(6).

After inspection of corroded strands, it was found that wire-unit section losses were different between strands even though their strand-unit section losses were very similar. The fracture of a strand, uniaxial material, will be occur at the most corroded wire (it was observed in tensile test), therefore, relation between wire-unit section loss and strand-unit section loss should be taken into

Preprints (www.preprints.org) | NOT PEER-REVIEWED | Posted: 20 May 2020 doi:10.20944/preprints202005.0324.v1

Peer-reviewed version available at Appl. Sci. 2020, 10, 4055; doi:10.3390/app10124055

account for criteria of corrosion evaluation. Fig. 8 shows the relation between the maximum wire corrosion and the section loss of the corresponding strands for the inspected specimen. The figure also shows the number of corroded wires in the strand. If the number of corroded wires is two, for example, the strand consists of two corroded wires and five non-corroded wires. The maximum number of corroded wires is six because the remaining wire (core wire) is impossible to inspect.

In Fig. 8, two tendencies can be observed. First, a higher number of corroded wires tends to correspond to a higher section loss in the wire as well as in the strand. A higher strand-unit section loss is a natural result, because the strand-unit section loss is the sum of the wire-unit section losses. However, the higher levels of corrosion in the wires have a special meaning, which is that the corrosion reactions continue to occur in some wires, and once a certain level of corrosion occurs, other wires also begin to corrode. Because a plurality of strands is bundled together in one tendon due to tension, the inner wires are better protected from corrosion; therefore, the inner wires corrode sequentially after the outer wires are sufficiently corroded.

In addition, a higher number of corroded wires tends to produce more widely scattered data. This means that pitting corrosion can develop differently in the wires; therefore, the maximum wire-unit corrosion in a strand can be very different between corroded strands even though they have the same level of strand-unit corrosion. If the strand fracture is defined as the moment of a single wire fracture [15], it is necessary to consider the cross-sectional loss in the wire after at least a 2% section loss in a strand.

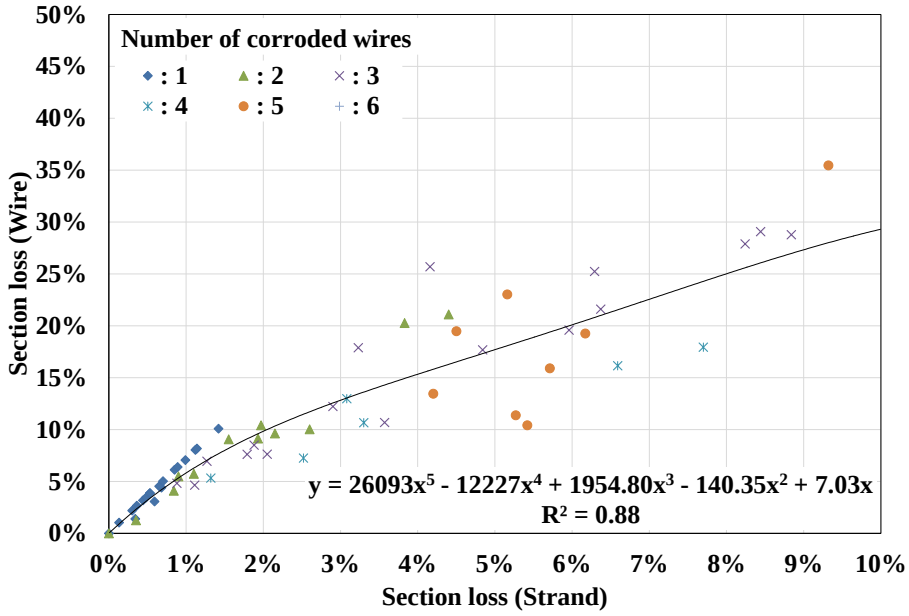

Figure 8. Relation between section loss of strands and the most corroded wire

3.2. Tensile test of corroded strands

A tensile test was conducted with a universal testing machine as shown in Fig. 9(a). The specimens were loaded to their failure using the displacement control method with a speed of 5 mm/min, and the two ends of the strand were held by the grip. Among the strands extracted from the bridge, three non-corroded strands were defined as reference specimens for the 15.2 and 12.7 types. Table 1 lists the mechanical properties of the non-corroded strands as averages of the test results from the three specimens.

Strands with no or little corrosion showed failures of all the wires fracturing at the same moment as shown in Fig. 9(b). For the corroded strands, shown in Fig. 9(c), the most corroded wire fractured earlier than the other wires. Owing to the fracture of the wire, the strand's strength suddenly decreased; however, the remaining wires maintained a structural capacity until the next wire was fractured as shown in Fig. 10(a). Furthermore, the amount of load reduction between the moments of

Preprints (www.preprints.org) | NOT PEER-REVIEWED | Posted: 20 May 2020 doi:10.20944/preprints202005.0324.v1

Peer-reviewed version available at Appl. Sci. 2020, 10, 4055; doi:10.3390/app10124055

the first and second fractures was $^1/_7 f_{pu}$. This means the load was evenly carried by the seven wires, and the most corroded wire fracture earlier than the others. In this study, therefore, the failure event of the strand was defined as the moment when even one wire was broken, and the corresponding strength and strain were used for defining the ultimate strength and strain.

Table 1. Mechanical properties of the non-corroded strand

Strand	Nominal sectional area (mm^2)	0.2% proof stress f_{py} (MPa)	Strain corresponding to 0.2% proof stress, ε_{py}	Ultimate strength, f_{pu} (MPa)	Ultimate strain, ε_{pu}
15.2 type	138.7	1,726	0.0099	1,865	0.075
12.7 type	98.71	1,135	0.0090	1,867	0.083

Fig. 10(b) shows samples of the test results from the test specimen. The elongation and maximum load due to the fracture show significant differences among the specimens; however, the yield performances are similar. This is because even if one wire reaches the yield first due to a cross-sectional loss, the remaining wires carry the load until they yield.

(a) (b) (c)

Figure 9. (a) Test setup, (b) failure of non-corroded strand, and (c) failure of corroded strand

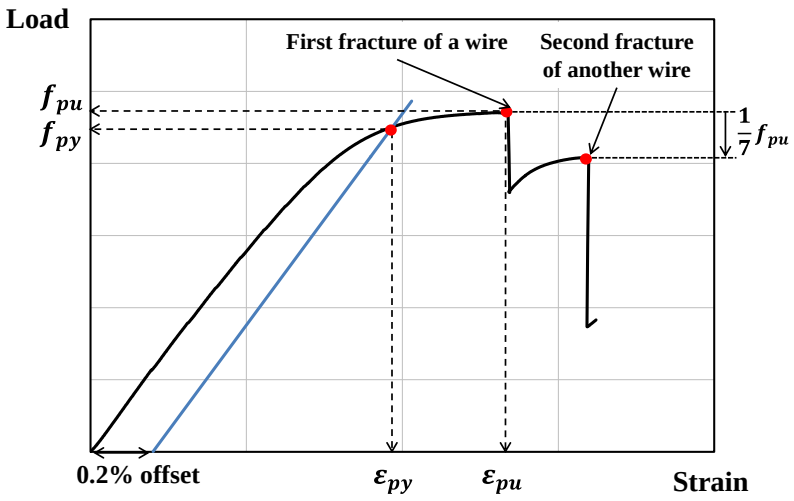

(a)

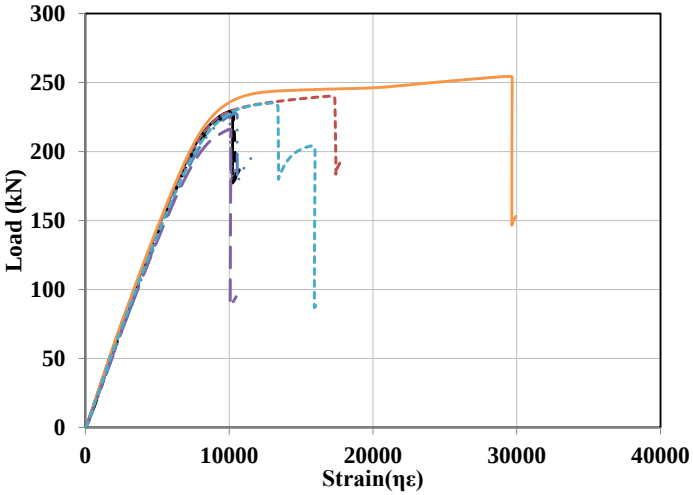

(b)

Figure 10. (a) Load-strain curve of a corroded strand and (b) samples from specimens

3.2. Residual mechanical properties from test result

In this study, the residual mechanical properties due to corrosion are defined as the relations between section loss and yield (or ultimate) strength. The section loss is explained under the strand-unit and wire-unit section losses. The reason the wire-unit section loss is considered is because of the assumption that the corrosion of a strand can be localized in a few of the 7 wires. A premature wire fracture due to corrosion would be the determining factor in the performance of the corresponding strand. This has been validated by the decrease in strength owing to wire-unit fracture as shown in the experiment (Fig. 9).

ASTM A416 [19] defines the yield load as a 1% extension or 10,000 με, and EC2 [20] defines it as a 0.1% proof stress. However, as the extracted strand used in this research was manufactured under the KS D 7002 [21] standard, the definition of yield is a 0.2% proof stress, and the yield strength of a corroded strand is defined as a 0.2% proof stress. Specimens with severe corrosion that did not show a ductility up to a 0.2% strain rate were excluded from the yield behavior graph.

Fig. 11(a) and Fig. 11(b) show the relation of the 15.2 type strand's section loss with its yield strength and yield strain, respectively. Fig. 11(c) and Fig. 11(d) show the relation of the 12.7 type strands' section loss with its yield strength and yield strain, respectively. The coefficient of determination, R^2, has a maximum value of 0.0409, which indicates that the regression analysis is ineffective and the correlation of two factors is very low. This means, with the section loss of 22.52% (the most corroded specimen), the yield strength and strain show no significant gap even under the increase in section loss, as explained in Fig. 9(b). However, Fig. 11(b), which includes numerous highly corroded strands, indicates that the yield strength is likely to decrease if the number of corroded wires and corrosion level are high. Fig. 12 shows the corroded strand's yield strength and strain according to the section loss of the most corroded wire within each strand. As shown in Fig. 11, the yield properties and level of corrosion from the most corroded wire also showed no significant correlation.

Preprints (www.preprints.org) | NOT PEER-REVIEWED | Posted: 20 May 2020 doi:10.20944/preprints202005.0324.v1

Peer-reviewed version available at Appl. Sci. 2020, 10, 4055; doi:10.3390/app10124055

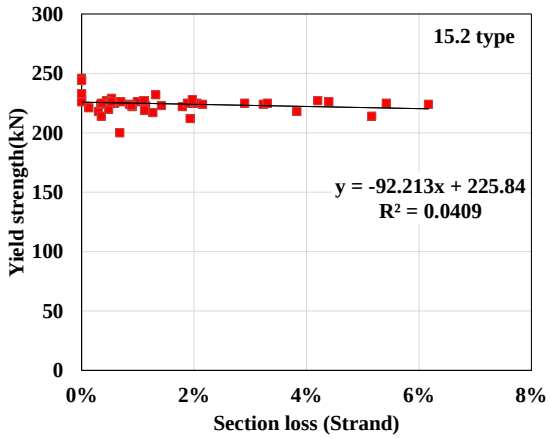

(a) Yield strength – Section loss relation (based on the strand)

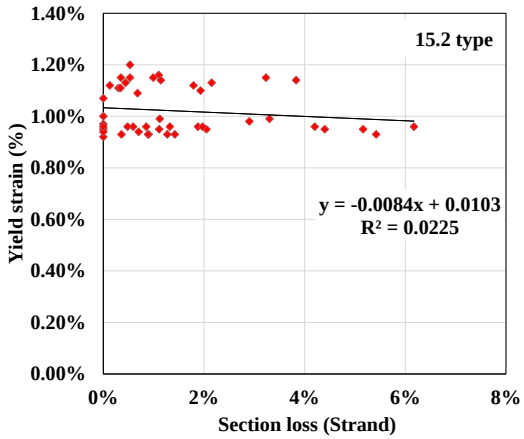

(b) Yield strain – Section loss relation (based on the strand)

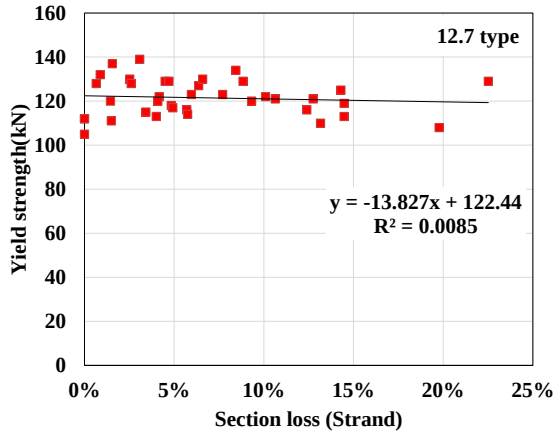

(c) Yield strength – Section loss relation (based on the strand)

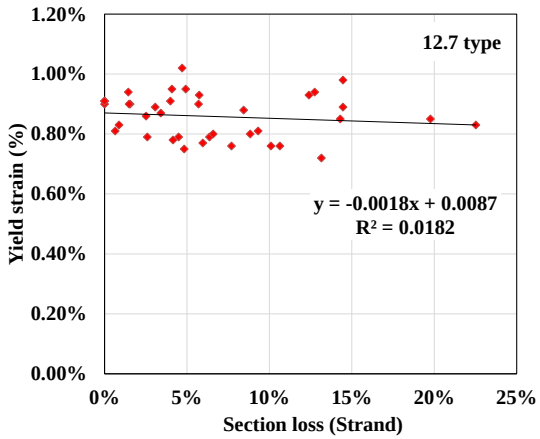

(d) Yield strain – Section loss relation (based on the strand)

Figure 11. Yield properties of corroded strands, evaluated with section loss of strands

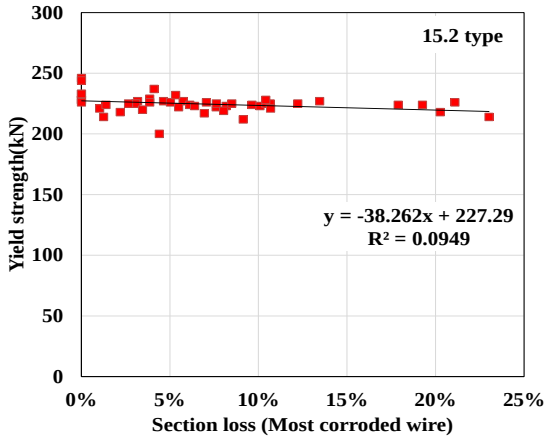

(a) Yield strength – Section loss relation (based on the most corroded wire)

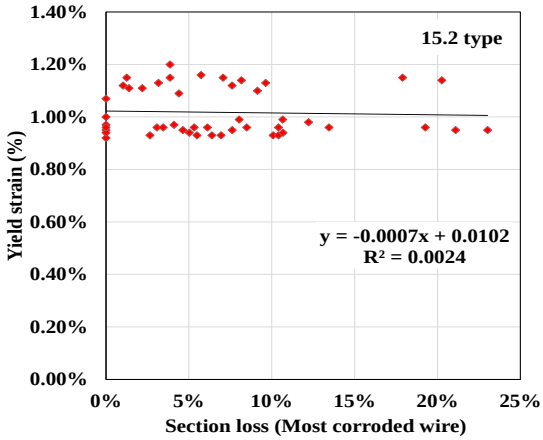

(b) Yield strain – Section loss relation (based on the most corroded wire)

Preprints (www.preprints.org) | NOT PEER-REVIEWED | Posted: 20 May 2020 doi:10.20944/preprints202005.0324.v1

Peer-reviewed version available at Appl. Sci. 2020, 10, 4055; doi:10.3390/app10124055

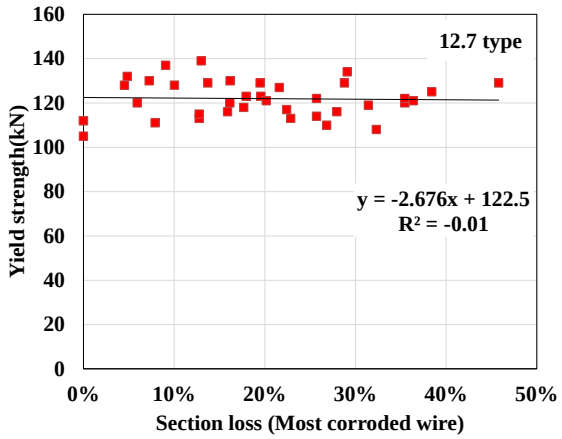

(c) Yield strength – Section loss relation (based on the most corroded wire)

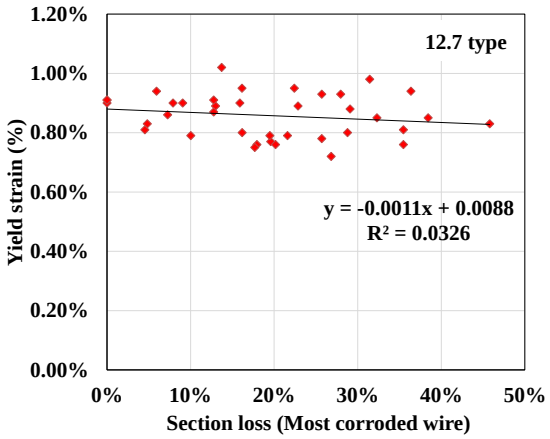

(d) Yield strain – Section loss relation (based on the most corroded wire)

Figure 12. Yield properties of corroded strands, evaluated with the section loss of the most corroded wire in each strand

Before evaluating the ultimate behavior of the corroded strands, as the two strands have different ultimate strengths, to compare them, the ultimate strength was normalized through the calculation of P_u/P_0. P_uu refers to each corroded strand specimen's ultimate strength, and P_0 refers to the ultimate strength of a non-corroded strand. P_0, ultimate loads from f_{pu} in Table 1, are 261.20 kN and 184.28 kN, for 15.2 type and 12.7 type, respectively. If P_u/P_0 is equal to 1.0, it means the strand's strength did not decrease.

Figs. 13(a) and (b) show the relations between the strand-unit section loss and the ultimate strength and strain. As the graph indicates, unlike for the yield strength, the two factors seem to be correlated. Furthermore, the decrease in ultimate strain can be a worse problem than the decrease in strength. For example, for a 5% section loss, a 20% maximum strength loss can occur; however, in the case of ultimate strain, for a 5% section loss, an 85% maximum decrease in deformation capacity can occur.

Regarding the test results, the strength of the non-corroded strands (P_u/P_0=1) and ultimate strain (7.89%, average of the ultimate strain of the two types listed in Table 1) were set as the axis and intercept, and a regression analysis was conducted. The ultimate strain showed a high deviation implying a low credibility of the index regression analysis result (R^2 = -0.015). Furthermore, there were specimens that showed similar strengths and ultimate strains despite having highly varying degrees of corrosion. The reason for such deviations in the test result distribution may be due to highly localized corrosion pits.

Errors occurred in the process of measuring the section loss due to corrosion, and specifically in deciding the location of the maximum depth pit by inspection and in measuring due to the intercept of the near wire and curvature of the spiral wire. The stress was concentrated in the damaged part due to the irregular surface condition of the corrosion pits [22]. This is the factor that causes the most difficulty in quantifying the corrosion property. The most corroded wire can determine the behavior of the corresponding strand. This is indicated by the terraced behavior shown in Fig. 9(a), and it seems more valid to measure the wire-unit section loss rather than the strand-unit section loss.

Figs. 13(c) and (d) show the section losses converted from the strand-unit to the wire-unit with the largest section loss within the strand. The explanatory power of the regression analysis increased from R^2 = -0.015 to R^2 = 0.3472. Figs. 12(c) and (d) show the lower limit curves with a 95% reliability and ± 2σ of the performance distribution depicting the relations of the wire-unit section losses with the ultimate strength and strain. It was assumed that the test result follows a normal distribution with the regression analysis curve as the average.

According to lower limit curve of 95% reliability, the ultimate strength proportionally decreased in relation to the maximum corroded wire section loss. The ultimate strength decreased by 20% and 38% when the section losses were 20% and 40%, respectively. Furthermore, the ultimate strain of the

Preprints (www.preprints.org) | NOT PEER-REVIEWED | Posted: 20 May 2020 doi:10.20944/preprints202005.0324.v1

Peer-reviewed version available at Appl. Sci. 2020, 10, 4055; doi:10.3390/app10124055

corroded strand at the lower limit curve of 95% reliability cannot meet the requirement of the minimum tensile strain (3.5%) from KS D 7002 [21] if the section loss exceeds approximately 4%. The ultimate strain is evaluated as 0 when the section loss is approximately 17%.

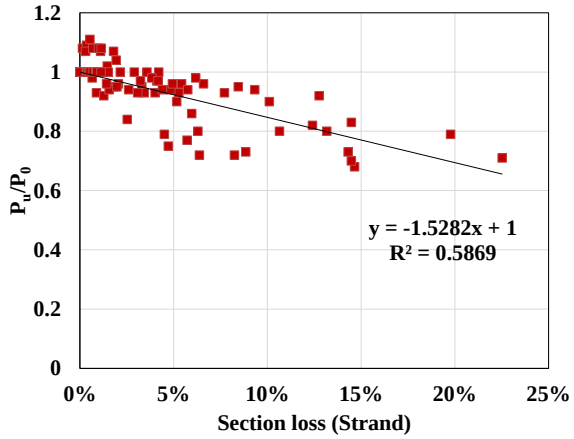

(a) Ultimate load – section loss relation (based on strand)

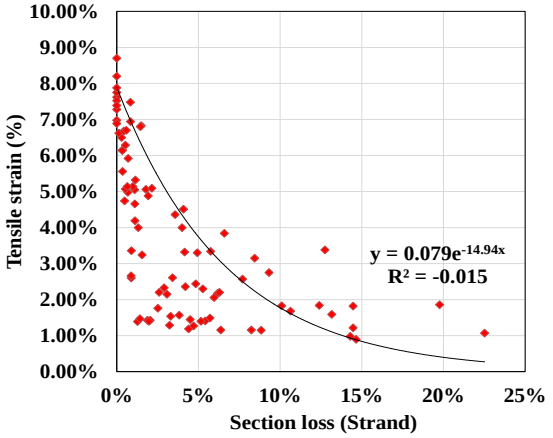

(b) Ultimate strain – section loss relation (based on strand)

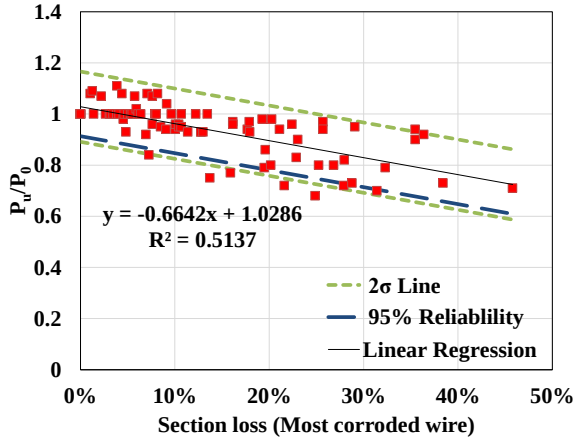

(c) Ultimate load – section loss relation (based on most corroded wire)

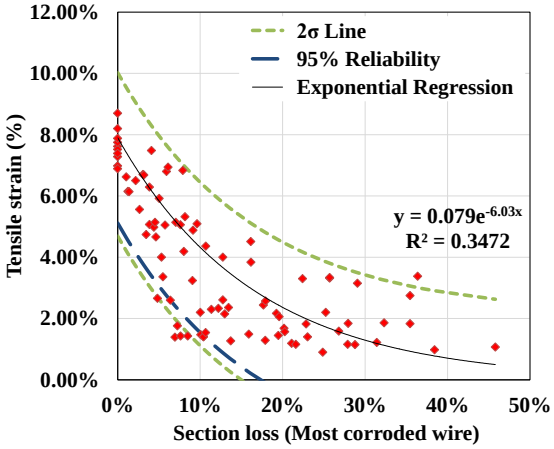

(d) Ultimate strain – section loss relation (based on most corroded wire)

Figure 13. Ultimate properties of corroded strands

The equations for the lower limit curve with a 95% reliability shown in Fig. 13(c) and (d) are as follows:

$$\frac{F_{c.pu}}{F_{pu}} = -0.6642\eta + 0.913, \tag{8}$$

$$\varepsilon_{c.pu} = \varepsilon_{pu} e^{-6.03\eta} - 0.0278 \tag{9}$$

where F_{pu} and $F_{c.pu}$ are the ultimate loads of the non-corroded and corroded strands in kN, respectively. ε_{pu} and $\varepsilon_{c.pu}$ are the ultimate strains of the non-corroded and corroded strands, respectively. η is the section loss according to Eq. (7).

Preprints (www.preprints.org) | NOT PEER-REVIEWED | Posted: 20 May 2020 doi:10.20944/preprints202005.0324.v1

Peer-reviewed version available at Appl. Sci. 2020, 10, 4055; doi:10.3390/app10124055

4. Prestressed concrete beams with corroded strands

4.1. Test specimen

To observe the behavior of the corroded strands in a prestressed concrete member, four simply supported beam specimens were manufactured and tested. The dimensions and details of the specimens are presented in Fig. 14. The post tensioned beams had a section of 150 × 220 × 2000 mm with a single 7-wire Φ15.2 mm strand.

Table 2 lists the information on the material and strands' corrosion status for the four manufactured PSC beam specimens. Strands used in the test beams were artificially corroded through exposure to NaCl (to create humid and dry conditions in cycles) at a certain location for several months as shown in Fig. 14(a). The corroded strands have very similar corrosion shape to the actual corrosion shape observed from existing bridge B (Fig. 2) in the 0-10% range of section loss. Before the corroded strands were introduced to the test beams, section loss had been evaluated by Eqs. (1) – (6). The RB specimen ID refers to the reference member without corrosion. QB refers to a member with corrosion at 1/4 of the span length (450 mm from the support), and MB refers to the member with corrosion in the center of the span length.

The average yield, ultimate strength, and elastic modulus of the prestressing steel were 1,630 MPa, 1,865 MPa, and 194.5 GPa, respectively. The yield and ultimate strength of the deformed bar were 400 MPa and 560 MPa, respectively. The concrete was manufactured to have a compressive strength of 40 MPa, and the average compressive strength was 44.07 MPa when the experiment was conducted. Regardless of corrosion status, the effective prestress force on the strands was equally applied as 160 kN.

Flexural tests were performed using the displacement control method under a 4-point loading condition. The span length of the specimen was 1,800 mm, and the loading position was 600 mm from a support. Loadings were added until the compressed concrete reached a crushing state even if the strand fractured earlier due to corrosion.

(a)

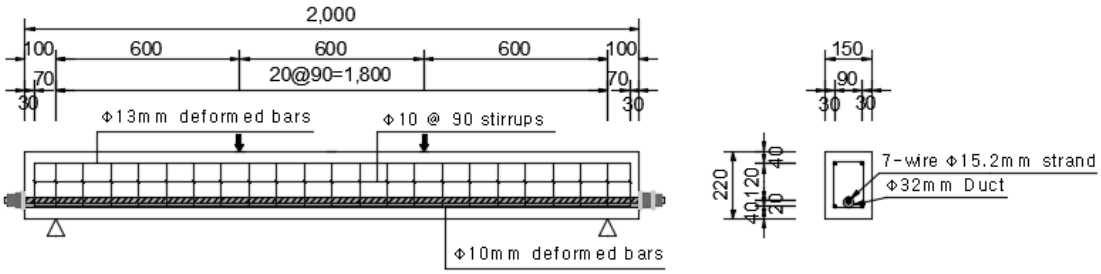

(b)

Figure 14. (a) Test setup and (b) detail drawing

Preprints (www.preprints.org) | NOT PEER-REVIEWED | Posted: 20 May 2020 doi:10.20944/preprints202005.0324.v1

Peer-reviewed version available at Appl. Sci. 2020, 10, 4055; doi:10.3390/app10124055

Table 2. Beam test specimens

ID	Location of corrosion	Section loss (strand)	Section loss (most corroded wire)	Effective prestressing force	Material properties
RB	-	0 %	0 %	160 kN	Concrete: 44.07 MPa Yield strength (rebar): 400 MPa Tensile strength (rebar): 560 MPa Yield strength (strand): 1630 MPa Tensile strength (strand): 1865 MPa Elastic modulus of strand: 194.5 GPa
QB	1/4	4.82 %.	21.56 %.		
MB1	1/2	6.67 %	22.24 %		
MB2	1/2	7.51 %	18.89 %		

4.2. Test result

Fig. 15 shows the load-displacement curves of the specimens and an image of the wire fracture after the tests were conducted. Table 3 summarizes the strength, displacement, and failure mode of the specimens. Considering the material properties in Table 2, the non-corroded RB's nominal strength was 159.3 kN. The strength and displacement in the experiment was 163.9 kN and 18.40 mm, respectively. After the yielding of the strand and rebar, the compressed concrete reached a crushing failure mode. After the QB member experienced one wire fracture, it then reached a crushing failure. The strength and displacement at the moment of fracture was 161.0 kN and 17.89 mm, respectively. The corrosion reduced the strength and flexural capacity by 1.77% and 2.77% compared to the RB member. This means that the corroded strand had a limited influence on the strength of the member due to sufficient bond between the strand and surrounding grout.

MB1 and MB2, which had corrosion in the center of the span length, showed strength decreases of 10.68% and 17.27% and decreases in the displacement capacity of 12.28% and 13.15%, respectively. Both specimens experienced a compression failure after two wire fractures. Additionally, four wires failed in MB2, which means several wires can fail at one time. The corrosion in the strands at the location of the maximum moment significantly influences the ultimate behavior of a PSC beam.

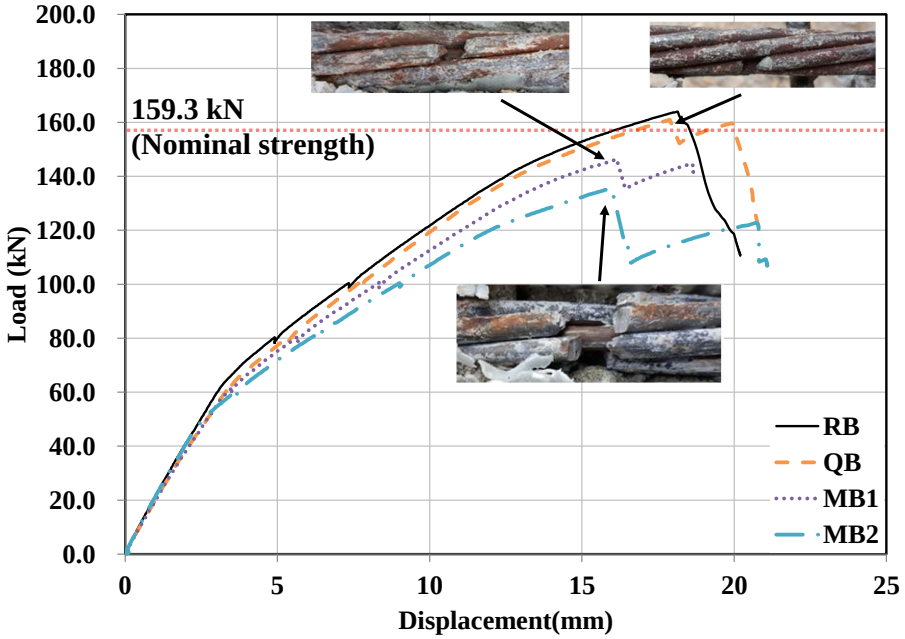

Figure 15. Load-displacement curves of PSC beam specimens

Preprints (www.preprints.org) | NOT PEER-REVIEWED | Posted: 20 May 2020 doi:10.20944/preprints202005.0324.v1

Peer-reviewed version available at Appl. Sci. 2020, 10, 4055; doi:10.3390/app10124055

Table 3. Test results of PSC beam specimens

ID	Maximum load (kN)	Load reduction ratio to RB	Maximum disp. (mm)	Disp. reduction ratio to RB	Failure mode
RB	163.9	-	18.40	-	Compressive concrete crush
QB	161.0	1.77 %	17.89	2.77 %	Compressive concrete crush after 1 wire fracture
MB1	146.4	10.68 %	16.14	12.28 %	Compressive concrete crush after 2 wire fracture
MB2	135.6	17.27 %	15.98	13.15 %	Compressive concrete crush after 2 wire fracture

4.2. Determination of the flexural strength of a corroded PSC beam

To calculate the flexural strength of a PSC beam, the approximate value of f_{ps}, which refers to the stress of the strand at the moment of the beam's failure, can be obtained from the design codes, or the strain compatibility method can be utilized to derive the value. According to ACI 318-14 [23], Eq. (10) is the approximate expression for f_{ps}. $f_{c.ps}$ and $\rho_{c.p}$ refer to the ultimate strength of the corroded strand and steel ratio, respectively. The section loss by corrosion can be calculated from Eqs. (1) – (6), and the decreased ultimate strength can be calculated using Eq. (7) and Eq. (8) along with the result of tensile tests given in Fig. 16.

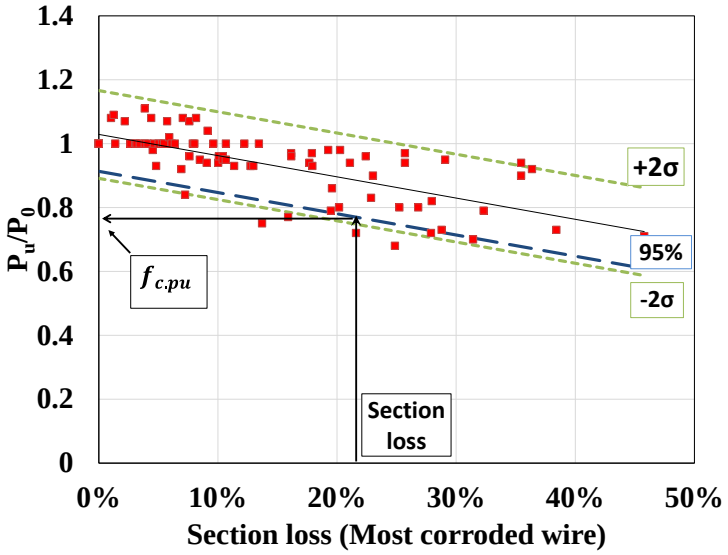

Figure 16. Determination of $f_{c.ps}$ from 95% lower reliability limit of ultimate strength

$$f_{c.ps} = f_{c.pu}\left[1 - \frac{\gamma_p}{\beta_1}\left\{\rho_{c.p}\frac{f_{c.pu}}{f_{ck}} + \frac{d}{d_p}(\omega - \omega')\right\}\right], \quad (10)$$

where

$f_{c.ps}$: Stress of the corroded prestressing strand when the beam fails

$f_{c.pu}$: Ultimate stress of the corroded prestressing strand

$f_{c.pu}$: Coefficient according to the type of strand $\begin{cases} 0.55 \; when \; f_{py}/f_{pu} \geq 0.80 \\ 0.40 \; when \; f_{py}/f_{pu} \geq 0.85 \\ 0.28 \; when \; f_{py}/f_{pu} \geq 0.90 \end{cases}$

β_1: Ratio between the depth of an equivalent rectangular concrete stress block and the neutral axis depth (= a/c)

$\rho_{c.p}$: Corroded prestressing steel ratio $(= A_{c.p}/bd_p)$

d: Depth of tensile reinforcement

d_p: Depth of prestressing strand

ω: Tensile reinforcement index$\left(= \rho\frac{f_y}{f_{ck}},\ \rho = \frac{A_s}{bd}\right)$

ω ': Compression reinforcement index $\left(= \rho'\frac{f_y}{f_{ck}},\ \rho' = \frac{A_s'}{bd}\right)$

$f_{c.ps}$ from Eq. (10) for each specimen and the corresponding flexural strength are listed in Table 4. The RB, MB1, and MB2 specimens showed reasonable estimations of the strength, while QB showed a value different from the test value. The reason is that the cross section of corrosion is at 1/4 of the span length, such that a lesser flexural moment is carried than that occurring at the center. Therefore, the governing cross section for the nominal flexural strength becomes center (154.47 kN) rather than 1/4 (211.73 kN) even though the reduced $f_{c.ps}$ is considered. The failure mode, however, showed a wire fracture at the 1/4 of the span length. This means that the reduced ultimate strain of the corroded strand can be the governing factor of the flexural strength. To consider this, the strain compatibility method should be used.

Although MB2 showed a lower flexural strength of 135.6 kN than that of MB1 at 146.4 kN, the flexural strength calculated by Eq. (10) was higher (138.53 kN < 140.6 kN). This is because MB2's maximum wire-unit section loss of the corroded strand was lower than that of MB1 (18.89% < 22.24%), making the fps from Eq. (10) a lesser value than that of MB1 (1289 MPa < 1327 MPa). This phenomenon was caused from an uncertainty in the tensile behavior as well as an undefined bonding behavior of the corroded strand. Therefore, a further study is required to explain this behavior.

Table 4. Flexural strength evaluation using approximated determination of fps with eq. (10)

ID	Ultimate strength of corroded strand based on 95% lower reliability limit	$f_{c.ps}$ from Eq. (10)	Maximum load (test)	Maximum load considering Eq. (10)	Differnce
RB	1860 MPa	1614 MPa	163.9 kN	154.47 kN	- 5.75 %
QB	1432 MPa	1293 MPa	161.0 kN	154.47(211.73*) kN	- 4.06 %
MB1	1423 MPa	1289 MPa	146.4 kN	138.53 kN	-5.38 %
MB2	1469 MPa	1327 MPa	135.6 kN	140.6 kN	3.69 %

* Ultimate load for the section at corrosion (1/4 of span length)

5. Conclusion

In this study, a total of 86 7-wire strands taken from existing bridges were investigated for section loss due to corrosion. The mechanical properties of the corroded strands derived from a 95% lower reliability curve were estimated by tensile tests. The flexural behaviors of four corroded PSC beams with different levels and locations of corrosion were also introduced. A method to evaluate flexural strength using an approximated $f_{c.ps}$ calculation was suggested. The conclusions of this study are as follows.

The higher number of corroded wires in one strand tends to have higher level of corrosion (section loss) of the wire. This indicates that the corrosion reactions continue to occur in some wires, and once a certain level of corrosion occurs, other wires also begin to corrode. Since a plurality of strands are bundled together in one tendon due to tension, the inner wires are protected from

corrosive condition compared to the outermost wires, therefore, inner wires are sequentially corroded after the outer wires are sufficiently corroded.

1) A higher number of corroded wires in one strand tends to have a higher level of corrosion (section loss) in the wire. This indicates that the corrosion reactions continue to occur in some wires, and once a certain level of corrosion occurs, other wires also begin to corrode. Because a plurality of strands is bundled together in one tendon due to tension, the inner wires are protected from corrosive conditions as compared to the outermost wires; therefore, inner wires corrode sequentially after the outer wires are sufficiently corroded.
2) The maximum wire-unit corrosion in a strand can be very different between corroded strands even though they have the same level of strand-unit corrosion. If the strand fracture is defined as the moment a single wire fractures, it is necessary to consider the cross-sectional loss in the wire, after at least a 2% section loss of a strand.
3) Within the section loss of 22.52% (the most corroded specimen), the yield strength and strain shows no significant gap even under the increase of section loss, because even if one wire reaches a yield first due to cross-sectional loss, the remaining wires can carry the load until they yield. However, the yield strength is likely to decrease if the number of corroded wires and corrosion level are high.
4) The ultimate strength and strain for the corroded strand are introduced by the lower limit curve of 95% reliability from the tensile test result. The ultimate strength proportionally decreases; the ultimate strength decreased by 20% and 38%, when the section losses were 20% and 40%, respectively. The ultimate strain of the corroded strand cannot meet the requirement of minimum tensile strain (3.5%) from KS D 7002 [21] if the wire-unit section loss exceeds approximately 4%. The formulas for the lower limit curve of 95% reliability are also introduced.
5) Based on the test results of the PSC beam specimens with a single corroded strand, a method to evaluate the flexural strength using $f_{c.ps}$ is suggested. The proposed method shows an approximate estimate of flexural strength with a difference of 4.72% on average; however, it is limited to considering the rapid reduction of the ultimate strain of corroded strands.

A further study is required for the following issues. This study considers the single-strand PSC beam, and the flexural behavior can differ from that of multi-strand PSC beams. In addition, there is a limit in reflecting the ultimate strain reduction of corroded strands in the flexural strength evaluation. A strain-compatibility method can be adopted to solve these issues.

Author Contributions: "Conceptualization, C.-S.S.; methodology, C.-S.S. and C.-H.J.; validation, C.-H.J.; formal analysis, C.-H.J.; investigation, C.-H.J. and C.D.N; resources, C.-H.J. and C.D.N; data curation, C.-H.J.; writing—original draft preparation, C.-H.J.; writing—review and editing, C.-H.J.; visualization, C.-H.J.; supervision, C.-S.S; project administration, C.-H.J.; funding acquisition, C.-S.S. All authors have read and agreed to the published version of the manuscript."

Funding: This study was supported by a grant (18SCIP-B128570-02) from the Smart Civil Infrastructure Research Program funded by the Ministry of Land, Infrastructure and Transport (MOLIT) of the Korean government and the Korea Agency for Infrastructure Technology Advancement (KAIA)

Acknowledgments: This study was supported by a grant (18SCIP-B128570-02) from the Smart Civil Infrastructure Research Program funded by the Ministry of Land, Infrastructure and Transport (MOLIT) of the Korean government and the Korea Agency for Infrastructure Technology Advancement (KAIA)

Conflicts of Interest: "The authors declare no conflict of interest."

References

1. VDOT. EVALUATION OF GROUT AND STRANDS AT 13 TENDON LOCATIONS AND SELECTED VERTICAL PT BARS AT FIXED PIERS: Maintenance and Repair using Corrosion Mitigation Systems (Final Report). Virginia Department of Transportation; 2013

2. D Trejo, MBD Hueste, P Gardoni, RG Pillai, K Reinschmidt, SB Im, S Kataria, S Hurlebaus, M Gamble, TT Ngo. Effect of Voids in Grouted Post-Tesioned Concrete Bridge Construction: Electrochemical testing and Reliability Assessment. Austin: Texas Transportation Institute; 2009.
3. Carsana M, Bertolini L. Corrosion failure of post-tensioning tendons in alkaline and chloride-free segregated grout: a case study. Structure and Infrastructure Engineering 2015; 11(3): 402-411
4. 陸賢, 田中泰司, 山口貴幸, 下村匠. 腐食した PC より線の機械的性質とプレテンション PC 梁の残存耐力の評価 (Evaluation of mechanical properties of corroded PC strand and residual strength of pre-tensioned PC beam). Proceedings of the Symposium on Developments in Prestressed Concrete 2012; 21: 211-216 (in Japanese).
5. Wu X, Li H. Effect of Strain Level on Corrosion of Prestressing Steel Strands. Proceedings of International Association for Bridge and Structural Engineering; Zurich. Switzerland; 2016.p 292–299.
6. Rinaldi Z, Imperatore S, Valente C. Experimental evaluation of the flexural behavior of corroded P/C beams. Construction and Building Materials. 2010; 24: 2267-2278
7. ASTM G1-03. Standard Practice for Preparing, Cleaning, and Evaluating Corrosion Test Specimens. ASTM International, West Conshohocken, PA; 2017
8. ASTM G49-94. Standard Guide for Examination and Evaluation of Pitting Corrosion1.ASTM International, West Conshohocken, PA; 2005
9. Reis R A. Corrosion Evaluation and Tensile Results of Selected Post-Tensioning Strands at the SFOBB Skyway Seismic Replacement Project. Sacramento: California Department of Transportation; 2007
10. Lu ZH, Li F, Zhao YG. An Investigation of Degradation of Mechanical Behaviour of Prestressing Strands Subjected to Chloride Attacking. Proceedings of International Conference on Durability of Concrete Structures; 2016 Jun 30-Jul 1; Shenzhen University, Shenzhen, Guangdong Province: P.R.China; 2016.
11. Val DV, Melchers RE. Reliability of Deteriorating RC Slab Bridges. Journal of Structural Engineering.ASCE.1997; 123(12): 1638-1644.
12. Stewart MG. Mechanical behaviour of pitting corrosion of flexural and shear reinforcement and its effect on structural reliability of corroding RC beams. Structural Safety.2009;31: 19-30.
13. Hartt WH, Lee SK. Projecting Corrosion-Induced Bridge Tendon Failure Resulting from Deficient Grout: Part I–Model Development and Example Results. CORROSION. 2016;72(8):991-998.
14. Yoo CH, Park YC, Kim HK. Modeling Corrosion Progress of Steel Wires in External Tendons. Journal of Bridge Engineering. 2018; 23(12)
15. Jeon CH, Lon S, Shim CS. Equivalent material model of corroded prestressing steel strand. Journal of Materials Research and Technology. 2019; 8(2): 2450-2460
16. Lee JB, Lee, YJ, Shim CS. Probabilistic prediction of mechanical characteristics of corroded strands. Engineering Structures. 2020; 203
17. KS F 2713. Testing method for analysis of chloride in concrete and concrete materials. Korean Agency for Technology and Standards. 2017 (in Korean)
18. KS L 5120. Testing method for chemical analysis of Portland concrete. Korean Agency for Technology and Standards. 2004 (in Korean)
19. ASTM A416 / A416M-18. Standard Specification for Low-Relaxation, Seven-Wire Steel Strand for Prestressed Concrete. ASTM International. West Conshohocken. PA. 2018
20. British Standards Institution. Eurocode 2 : design of concrete structures. British standard. London: BSi. 2008.
21. Korean Agency for Technology and Standards. Uncoated Stress-Relieved Steel Wires and Strands for Prestressed Concrete (KS D 7002). 2011. (in Korean).
22. Jones, D.A. Principles and Prevention of Corrosion. Macmillan Publishing Company, New York. 1992
23. ACI Committee 318. Building Code Requirements for Structural Concrete (ACI 318-14). 2015.